

# High-Accuracy Microwave Atomic Clock via Magic Optical Lattice

Xiaoji Zhou, Xuzong Chen, and Jingbiao Chen\*

*School of Electronics Engineering & Computer Science, Peking University,  
Beijing 100871, P. R. China*

(Dated: November 4, 2018)

A microwave atomic clock scheme based on Rb and Cs atoms trapped in optical lattice with magic wavelength for clock transition is proposed. The ac Stark shift of clock transition due to trapping laser can be canceled at some specific laser wavelengths. Comparing with in fountain clock, the cavity related shifts, the collision shift, and the Doppler effect are eliminated or suppressed dramatically in atomic clock when the magic optical lattice is exploited. By carefully analyzing various sources of clock uncertainty, we conclude that a microwave atomic clock with an accuracy of better than  $2 \times 10^{-17}$  is feasible, which is of the same accuracy as the expected best optical atomic clock.

PACS numbers: 06.30.Ft, 06.20.-f, 32.80.Qk, 32.30.Bv

After the realization of Zacharias' idea of atomic fountain [1], many advances in high-precision measurement physics, including the test of fundamental constants stability [2, 3], have been achieved with atomic fountain clock with a total fractional uncertainty of  $3.5 \times 10^{-16}$  [2, 3, 4, 5]. On the other hand, many critical improvements of optical atomic clock [6, 7, 8, 9, 10] in the past several years indicate that a potential competitor with much better uncertainty than the microwave atomic clocks will soon be the new generation of atomic clocks. For example, various experimental schemes of optical clock based on alkaline-earth atoms and Yb atoms with an uncertainty of better than  $2 \times 10^{-17}$  are proposed [10, 11, 12, 13]. Except the active optical clock [11], all passive optical clock schemes use neutral atoms trapped in optical lattices formed by "magic" wavelength, which can be used to adjust the ac Stark shift of clock transition as fine as  $1 \times 10^{-3}$ Hz [8, 9, 10]. Advantages of single ion clock and the conventional neutral atom clock are combined there since millions of neutral atoms are trapped within Lamb-Dick regime for long time clock-laser interrogation. The most recent evaluation of atomic fountain clock is one order of magnitude better than that of the best achieved optical clock [6, 7]. However, it is obvious that, in atomic fountain configuration with laser cooled Cs and Rb, to reach a fractional uncertainty of microwave frequency standard to the level of  $1 \times 10^{-17}$  is a real technical challenge. Difficulties mainly arise from the effects of second-order Zeeman effect, collisions between the Cs atoms, microwave cavity, atomic motion and blackbody radiation. For microwave clock transition, it has been preliminarily precluded the possibility that a blue-detuned dipole trap will supersede a fountain due to hundreds of mHz residual ac Stark shift of clock transition in Na atom experiment [14, 15].

However, in this letter, we present the magic wavelengths for  $^{133}\text{Cs}$  and  $^{87}\text{Rb}$  clock transitions. Our calculations show that the ac Stark shift of Cs and Rb

clock transitions can be canceled at some specific magic wavelengths of trapping laser. Based on a careful analysis of various sources of clock uncertainty between fountain and lattice configurations, we conclude that a microwave atomic clock based on Cs and Rb atoms trapped in magic wavelength lattices is able to reach an accuracy of  $2 \times 10^{-17}$ .

To realize such a microwave clock in optical lattices, it is essential that the polarizabilities of the two clock states are matched to high accuracy at the magic wavelength. The frequency shift of clock transition induced by the axially symmetric electric field  $E_z$  with gradient  $E_{zz}$  of the lattice laser is described as [16],

$$\delta\nu = -\frac{1}{2}(\delta\alpha/h)E_z^2 - \frac{1}{4}(\delta C/h)E_{zz}^2 - \frac{1}{4}(\delta B/h)E_z^2 E_{zz} - \frac{1}{24}(\delta\gamma/h)E_z^4 \dots, \quad (1)$$

where  $h$  is the Planck constant,  $\delta\alpha$ ,  $\delta C$ ,  $\delta B$  and  $\delta\gamma$  are the difference of the dynamic dipole polarizabilities, quadrupole polarizabilities, dipole-dipole-quadrupole hyperpolarizabilities and second dipole hyperpolarizabilities between two clock states [16].

When  $\delta\nu$  equals zero, we get the exact magic wavelength for trapping laser. We first consider the dominant term, the first one on the right hand of Eq.(1), which is determined by the differential polarizability  $\delta\alpha_0$  (both scalar and vector part) and the tensor part  $\delta\alpha_2$ . The ac Stark shift of atomic hyperfine state  $|n, J, F, m_F\rangle$  for  $\delta\alpha_0$  [18, 19, 20, 21, 22] is,

$$\delta\nu_i = -\frac{3\pi c^2 I_L}{2h} \sum_{i \neq j} \frac{A_{ij}}{\omega_{ij}^2 (\omega_{ij} - \omega)^2} (2J' + 1)(2F' + 1) (2F + 1) \left( \begin{matrix} F' & 1 & F \\ m'_F & p & -m_F \end{matrix} \right)^2 \left\{ \begin{matrix} J & J' & 1 \\ F' & F & I \end{matrix} \right\}^2, \quad (2)$$

where  $I_L = (\varepsilon_0 c/2)|E_z|^2$  is the intensity of the trapping laser,  $c$  the light velocity,  $A_{kj}$  the Einstein spontaneous coefficient, and the coefficients in round and curly brackets are the  $3J$  and  $6J$  symbol, respectively.

\*Electronic address: jbchen@pku.edu.cn

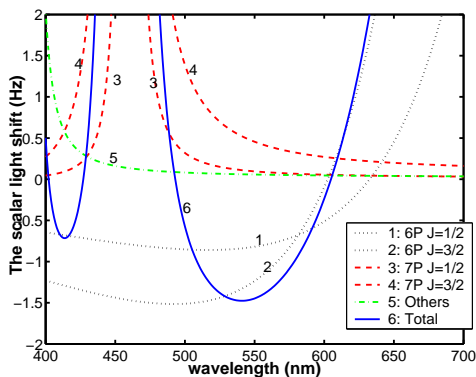


FIG. 1: The scalar light shift of Cs clock transition when atoms irradiated by a linearly polarized laser with intensity of  $10\text{kW}/\text{cm}^2$ .

They describe the selection rules and relative strengths of the transitions depending on the angular momenta, their projections  $m_F$ , the nuclear spin  $I$  and the polarization  $p = 0, \pm 1$  which stands for  $\pi$  and  $\sigma^\pm$  transition of related states. The primed quantum numbers refer to the excited states  $n'P_{J'}$  coupled to the ground state by allowed electric dipole transitions. We take the needed transition frequencies  $\omega_{ij}$  and  $A_{ij}$  coefficients from the collected data of Kurucz and Bell [23].

The scalar light shift of clock transition for Cs irradiated by a linearly polarized laser is shown in Fig.1. The ac Stark shift of Cs clock transition due to  $6P_{1/2}$  and  $6P_{3/2}$  states are negative at some wavelength region as the dotted lines show, but the contribution from  $7P$  as the dashed lines and higher states as the dash-dotted line are positive. The combination of the above shifts results in cancellation of ac Stark shift of Cs clock transition due to the linearly polarized trapping laser at some magic wavelengths. Our calculation predicts more than one magic wavelengths for Cs clock transition at 402.2nm, 427.0nm, 493.0nm, 604.8nm as showed in Fig.1 and for Rb at 370.4nm, 395.6nm, 452.3nm, 549.7nm which are labeled with cross-mark in Fig.2. The tuning rate  $(2\pi d\nu_{\text{clock}})/d\omega$  is as low as  $6 \times 10^{-14}$ . The depth of lattice trap is 167kHz ( $8\mu\text{K}$ ) for Cs with laser intensity of  $10\text{kW}/\text{cm}^2$  at wavelength of 604.8nm, and the vibrational frequency is about 34kHz.

If atoms are irradiated by  $\sigma^\pm$  laser, then  $p = \pm 1$  in Eq.(2), the consequent vector light shift of Cs and Rb clock transitions are shown in Fig.2. For  $^{87}\text{Rb}$  atom, the ac Stark shift due to  $\sigma^\pm$  light at the magic wavelength of  $\pi$  light is also very small, which is  $2.3 \times 10^{-3}$  Hz at 549.7nm with a laser power of  $10\text{kW}/\text{cm}^2$ . The magic wavelength of the vector light shift is 549.6nm, and its tuning rate  $(2\pi d\nu_{\text{clock}})/d\omega = 2.5 \times 10^{-14}$  are very close to that of the scalar light shift as mentioned above. But the vector light shift of Cs clock transition is much larger than that of  $\pi$  light. Considering a real 3D blue-detuned optical lattice, the trapped cold atom experiences not only the  $\pi$  light but also  $\sigma^\pm$  light. Thus for Cs,

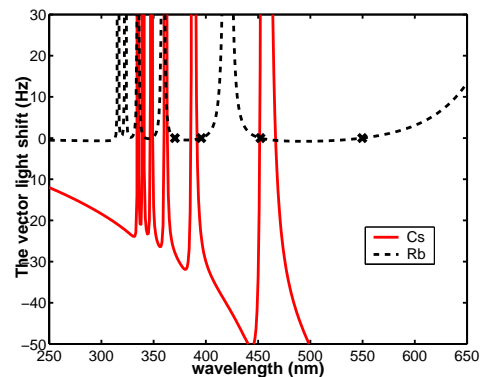


FIG. 2: The vector light shift of Cs and Rb clock transition when atoms irradiated by  $\sigma^\pm$  laser with intensity of  $10\text{kW}/\text{cm}^2$ .

the magic wavelength is mainly determined by the vector light shift. Even though, the tuning rate  $(2\pi d\nu_{\text{clock}})/d\omega$  is as low as  $1.5 \times 10^{-12}$  at a magic wavelength of 471nm for  $10\text{kW}/\text{cm}^2$  lattice laser intensity with 3D laser polarization configuration of  $E_x(\hat{e}_z), E_y(\hat{e}_z), E_z(\hat{e}_x)$ , and is good enough to control the light shift cancellation. It seems, considering the polarization,  $^{87}\text{Rb}$  is a better candidate than Cs to build a microwave atomic clock with atoms trapped in 3D optical lattice. The following analysis is based on Cs, but is also suitable for Rb.

The tensor light shift of clock transition  $\delta\alpha_2$ , arising from the third-order perturbation when the hyperfine interaction is taken into account [17], is roughly  $\delta_{hfs}/\delta$  of the  $\alpha$  term, where  $\delta_{hfs}$  is the hyperfine splitting of the coupled excited state and  $\delta$  is the trapping laser detuning of that state [9]. The tensor light shift of Cs clock transition is of the order mHz shown in Fig.3. The tuning rate  $(2\pi d\nu_{\text{clock}})/d\omega$  is as low as  $1 \times 10^{-19}$ , much smaller than that of scalar light shift, hence it only modifies the magic wavelength a little.

The static electric quadrupole polarizability  $C/h$ , dipole-dipole-quadrupole hyperpolarizability  $B/h$ , the second hyperpolarizability  $\gamma/h$  of Cesium ground state [16] are  $7.3 \times 10^{-25}\text{Hzm}^4/V^2$ ,  $4.65 \times 10^{-24}\text{Hzm}^4/V^3$ ,  $1.05 \times 10^{-24}\text{Hzm}^4/V^3$  respectively. Under the static field approximation, a  $10\text{kW}/\text{cm}^2$  trapping laser causes  $5 \times 10^{-5}\text{Hz}$ ,  $7.5 \times 10^{-6}\text{Hz}$  and  $2.5 \times 10^{-8}\text{Hz}$  shifts of clock transition corresponding to  $\delta C$ ,  $\delta B$ , and  $\delta\gamma$ , respectively. Atom is moving back and forth in the laser intensity minima of 3D blue-detuned lattice trap [14, 15] at the oscillating frequency of lattice, this effect results in the cancellation of shift due to  $\delta B$  term and negligible broadening due to  $\delta C$  term. These shifts are less than  $5 \times 10^{-8}\text{Hz}$  when the trapping laser power is stabilized to 0.1%. These shifts can also be compensated by scalar light shift easily. The ac Zeeman shift of clock transition is only about  $1 \times 10^{-10}\text{Hz}$  if the same laser power is assumed.

Fluctuations of the trapping laser intensity and frequency, scattering of the trapping light, and atomic

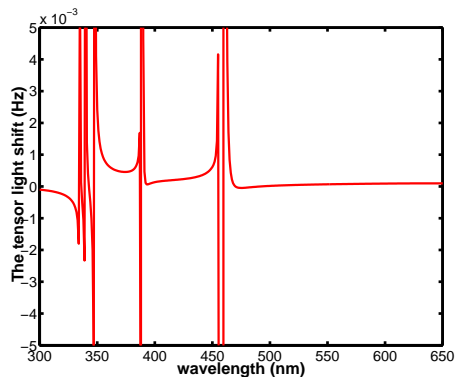


FIG. 3: The tensor light shift of Cs clock transition irradiated by linearly polarized laser with intensity of  $10\text{kW}/\text{cm}^2$ .

collisions with background atoms, which are the three mechanisms for heating atoms, mainly contribute to the trap lifetime. For the blue-detuned optical lattice trap, the atoms are trapped at the minima of laser intensity (the nodes of standing wave), the trap lifetime is larger than  $100\text{s}$ , since the Rayleigh scattering rate is about  $0.01\text{s}^{-1}$  and the Raman scattering rate is as low as  $5 \times 10^{-6}\text{s}^{-1}$  [22]. For the background pressure of the order of  $1 \times 10^{-11}\text{Torr}$ , the trap time can be more than  $300\text{s}$  [24, 25]. In the case when the lattice trapping laser is stable, the heating arising from laser intensity noise and beam pointing fluctuation [24, 25, 26] is negligible then the trap lifetime is finally limited only by Rayleigh scattering rate. The microwave pulses of clock transition are radiated by a dipole antenna close to the lattice position [14, 27]. The alternative method of clock transition interrogation is performed by Raman transition with microwave modulated laser.

We analyze the various sources of clock uncertainty with a comparison between fountain and lattice configurations as follows and list them in the Table I. In lattice clock configuration, considering atoms are confined within a very small size like  $(100\mu\text{m})^3$  for  $10^6$  atoms confined in lattice with lattice spacing of  $300\text{nm}$ , the temperature can be easily controlled to  $0.1\text{K}$ , thus the uncertainty of fractional blackbody shift is  $1.3 \times 10^{-17}$  or even better. Moreover, this  $100\mu\text{m}$  level location of atoms position results in a much better stability of gravitational redshift. But its uncertainty is determined only by the calibration of orthometric height of atoms position. This has potential applications in monitoring the change of gravitational potential due to moon or tide in real-time when the short-term stability is good. The spin-exchange collision shift in a Cs fountain clock is at the level of  $2 \times 10^{-14}$ , which can be corrected to as low as  $1 \times 10^{-16}$  [4] at low density. In lattice clock configuration using 3D lattice with less than unity occupation, the collision shift will be eliminated completely [9].

When a single microwave photon recoils during the Cs clock transition, the relative frequency shift is  $\Delta\nu_{\text{recoil}} = (\hbar k)^2 / (2M\hbar\omega) \approx 1.4 \times 10^{-16}$ , which was set as the

TABLE I: Comparison of uncertainties sources between fountain clock and expected lattice clock. All values are fractional frequency in  $10^{-17}$ .

Clock configuration	Fountain <sup>a</sup>	Lattice
Light shift(ac Stark shift)	0.001	<1, adjustable
Blackbody shift	26	1.3
Gravitational redshift	3	1
Collision shift	10	0
cavity pulling	1	0
Microwave recoil	14	0.1
Microwave leakage	20	0
cavity distributed phase	2	0
Microwave spectral purity	0.3	0.3
2 <sup>nd</sup> -order Zeeman	2	0.1
Majorana transition	2	0.1
Residual 1 <sup>st</sup> -Doppler	2	0
2 <sup>nd</sup> -order Doppler	2	$10^{-4}$
Rabi and Ramsey pulling	0.01	0.1
Bloch-Siegert	0.01	0.01
Background gas collision	0.1	0.1
The dc Stark effect	2	0.1
TOTAL UNCERTAINTY	38	2.0

<sup>a</sup>The reported minimal uncertainties of fountain clock. Residual 1<sup>st</sup>-Doppler is from [3], the cavity pulling and the second-order Doppler shift are from [28], microwave recoil is from [5], others are from [4].

uncertainty in a fountain clock [5]. In lattice, this recoil shift is within the spectral line width causing the residual 1st-order Doppler effect as analyzed below. Assuming the direction of microwave vector misalignment can be calibrated to  $\leq 1\text{mrad}$ , the microwave recoil shift can be calibrated to  $< 1 \times 10^{-18}$  in lattice clock. Microwave power-dependent shift including distributed cavity phase shift and microwave leakage shift is  $< 2 \times 10^{-16}$  [4] and cavity pulling is about  $1 \times 10^{-16}$  [28]. The shift due to majorana transition is expected less than  $2 \times 10^{-17}$ , which is set as uncertainty [4] in a fountain clock. While in the lattice clock, there is no cavity pulling when using the traveling microwave to interrogate the lattice-trapped atoms or via Raman process, and no majorana transition when the residual magnetic field fluctuation is much smaller than the C-field. Cavity phase shift [29] and microwave leakage shift can be eliminated since the Raman laser beam can be extinguished by mechanical shutter.

For Cs atoms, the second-order Zeeman shift due to effect of static magnetic field  $B_c$  in the unit of Gauss on clock transition is  $427 \times B_c^2\text{Hz}$ . The C-field in a fountain clock is about  $80\text{nT}=0.8\text{mG}$ , the uncertainty of fountain clock from C-field is  $2 \times 10^{-17}$  [4]. In the lattice clock configuration, since the atoms are confined within a very small size like  $(100\mu\text{m})^3$ , the requirement for magnetic field shielding and stability techniques will be dramatically relaxed, then the clock uncertainty from C-field  $B_c$  should be controlled less than  $1 \times 10^{-17}$  without any difficulty more than that of fountain clock.

This residual first order Doppler shift is from the prod-

uct of two vectors  $\vec{k} \cdot \vec{v}$ , where  $\vec{k}$  is the wave vector of microwave,  $\vec{v}$  is the atomic velocity. Assuming the direction misalignment is  $\leq 1\text{mrad}$ ,  $v = 3\text{m/s}$ , for a traveling wave, these parameters result in a frequency shift of  $0.02\text{Hz}$ . In a fountain, when the clock microwave signal is fed into the cavity “from the left” or “from the right”, the observed shift is about  $2.5 \times 10^{-5}\text{Hz}$  [3], this means the residual traveling wave component in the fountain cavity is near  $10^{-3}$  of the standing wave component. In a lattice clock, assuming with the same microwave intensity (the same pulse time about  $10\text{ms}$ ), the microwave is a pure traveling wave, thus it is 1000 times of the traveling wave in fountain cavity. And, the atomic average velocity during the microwave pulse period time  $10\text{ms}$  is  $\langle v \rangle = 0.2 \times 300\text{nm}/10\text{ms} = 6\mu\text{m/s}$ , where  $300\text{nm}$  is the lattice spacing,  $0.2$  means the atom is confined within the 20% central range near the center of a lattice trap, and  $10\text{ms}$  is the microwave pulse period. Considering the atomic motion within 3D lattice minima with a oscillating frequency during the microwave pulse period time  $10\text{ms}$ , the net effect of atomic ensemble is a Doppler spectral-broadening of  $\pm 2 \times 10^{-4}\text{Hz}$ . However, there is no net residual first-order Doppler shift in a lattice clock. The second-order Doppler shift due to relativistic time dilute is  $1 \times 10^{-17}$  [28] in a fountain clock, and will be  $< 1 \times 10^{-21}$  in lattice clock configuration. Rabi pulling, Ramsey pulling, microwave spectral purity, and Bloch-Siegert shift do not depend on the clock configuration, but they are determined by the C-field, the performance of synthesizer and other parameters for both clocks.

It is possible to reach  $N = 10^6$  of cold atoms for a lattice clock, therefore the stability can be improved to  $\sigma_y(\tau) = 5 \times 10^{-15}/\sqrt{\tau}$  assuming interrogation time is  $20\text{s}$ .

In summary, we have discussed the feasibility of a microwave atomic clock based on Rb and Cs atoms trapped in optical lattice with magic wavelength. By a careful comparison of various sources of clock uncertainty between fountain and lattice configurations, we conclude that a microwave atomic clock with an accuracy of  $2 \times 10^{-17}$  is feasible, which is of the same precision as the expected optical atomic clock. This clock scheme overcomes the formidable hurdles in fountain clock arising from the second-order Zeeman effect, collisions between the Cs atoms, the microwave cavity, the atomic motion and the blackbody radiation. Besides the potential application in high-precision measurements, our clock scheme promises that microwave based second definition in SI units can be realized one order of magnitude more precisely. Moreover, the practical size of microwave clock can be reduced to only one third of current fountain size or even smaller, and the idea in this letter is also applicable for designing primary atomic clock for international space station [3, 30].

We acknowledge helpful discussions with Yiqiu Wang and Ruoxin Li. We also thank Mei Zhang for her critical reading. This work is supported by MOST under Grant No.2005CB3724500, and NSFC under Grants 60178016, 10104002, 10574005.

- 
- [1] N. F. Ramsey, *Molecular Beams*, New York, Oxford University Press, 1956; Andrea de Marchi, *Metrologia* 18, 103(1982); P. Forman, *Proc. IEEE* 73, 111(1985); Kasevich M. A. Kasevich, E. Riis, S. Chu, and R. G. DeVoe, *Phys. Rev. Lett.* 63, 612(1989); R. Wynands and S. Weyers, *Metrologia* 42, S64(2005).
- [2] S.A.Diddams, J. C. Bergquist, S. R. Jefferts, C. W. Oates, *Science* 306, 1318 (2004).
- [3] S. Bize et al., *C. R. Physique* 5, 829 (2004).
- [4] T. P. Heavner et al., *Metrologia* 42, 411(2005).
- [5] C. Vian et al., *IEEE Tran. Instrum. Meas.* 54, 833(2005).
- [6] P. Gill, *Metrologia* 42, S125(2005).
- [7] H. S. Margolis et al., *Science* 306, 1355(2004).
- [8] A. D. Ludlow et al., arXiv:physics/0508041
- [9] H. Katori, M. Takamoto, V. G. Pal’chikov, V. D. Ovsiannikov, *Phys. Rev. Lett.* 91, 173003(2003).
- [10] M. Takamoto et al., *Nature* 435, 321 (2005).
- [11] J. Chen, arXiv:physics/0512096.
- [12] T. Hong et al., *Phys. Rev. Lett.* 94, 050801(2005).
- [13] R. Santra et al., *Phys. Rev. Lett.* 94, 173002(2005).
- [14] N. Davidson et al., *Phys. Rev. Lett.* 74, 1311(1995).
- [15] [http://www.weizmann.ac.il/home/davidson/abstract\\_dark\\_re30](http://www.weizmann.ac.il/home/davidson/abstract_dark_re30)
- [16] P. Fuentealba and O. Reyes, *J. Phys. B: At. Mol. Opt. Phys.* 26, 2245(1993).
- [17] C. Ospelkaus, U. Rasbach, and A. Weis, *Phys. Rev. A* 67, 011401(2003).
- [18] D. A. Steck, Cesium and Rubidium D line data, <http://steck.us/alkalidata>, 2003.
- [19] *The physics of laser-atom interactions* (Cambridge University press, 1997) 159.
- [20] R. Grimm, M. Weidemüller, Y. B. Ovchinnikov, *Adv. Atom. Mol. Opt. Phys* 42, 95(2000).
- [21] C. Degenhardt, H. Stoehr, U. Sterr and F. Riehle, *Phys. Rev. A* 70, 023414(2004).
- [22] M. V. Romalis, and E. N. Fortson, *Phys. Rev. A* 59, 4547(1999).
- [23] R. Kurucz, and B. Bell, 1995 Atomic line data, Kurucz CD-ROM.
- [24] K. M. O’Hara et al., *Phys. Rev. Lett.* 82, 4204(1999).
- [25] K. M. O’Hara, S. R. Granade, M. E. Gehm, and J. E. Thomas, *Phys. Rev. A* 63, 043403(2001).
- [26] M. E. Gehm, K. M. O’Hara, T. A. Savard and J. E. Thomas, *Phys. Rev. A* 58, 3914(1998).
- [27] S. Kuhr et al., *Phys. Rev. A* 72, 023406(2005).
- [28] K. Szymaniec et al., et al., *Metrologia* 42, 49(2005).
- [29] R. Li, and K. Gibble, *Metrologia* 41, 376 (2004).
- [30] <http://tf.nist.gov/timefreq/cesium/parcs.htm>;  
<http://www.esa.int/SPECIALS/GSP/SEM1AGZO4HD-0.html>.